Special Interest Group Meeting on Thermal Issues
ETH, Zurich, Switzerland, March 2022
www.euspen.eu

Limits of linear parametric models for thermal error compensation of a large grinding machine

Otakar Horejš[1], Martin Mareš[1]

[1]Czech Technical University in Prague, Faculty of Mechanical Engineering, Department of Production Machines and Equipment, RCMT, Horská 3, 128 00 Prague, Czech Republic

o.horejs@rcmt.cvut.cz

Abstract

The thermal errors of the machine tools are an important element in inaccuracies of the machined workpiece. In the past few decades, thermal errors implicated mainly by an individual source (e.g. spindle or environment), have been successfully reduced by software compensation techniques such as multiple linear regression analysis, finite element method, neural network, transfer function (TF) within similar calibration and verification conditions. An approach based on TFs is used for thermal error modelling in this research. Method respects basic heat transfer mechanisms in the MT structure, requires a minimum of additional gauges. The approach enables an insight into the share of individual sources in the total machine thermal error by combination of linear parametric models. The aim of this research is to investigate an applicability of thermal error compensation model of large grinding machine when the conditions (such as diameter of grinding wheel) are different during calibration and verification testing. Undesirable thermal errors in this case are caused by the operation of the wheel head. Models are composed for approximation of thermally induced relative displacements between static bodies of headstock (with clamped workpiece) and wheel head and between axes of rotation of those machine components. Limits of derived linear parametric models and its capability of industrial applicability are critically discussed in more detail.

Thermal error, Grinding machine, Linearity, Industrial applicability

1. Introduction

The heat generated, e.g. by moving axes and machining processes, creates thermal gradients, resulting in the thermal elongation and bending of machine tool (MT) elements, which substantially deteriorate MT accuracy. Consequently, up to 75% of all geometrical errors of machined workpieces are caused by temperature effects [1].

Thermal errors may be sufficiently reduced by new MT design concepts [2], ~~a~~daptive or intelligent control of cooling systems [3], integrated additional sensors in the MT structure [4] or direct (in-process) measurement techniques [5]. However, they do increase machine and operational costs and/or result in machining process interruptions and prolonged production time.

A very promising contemporary approach is the use of final element method (FEM) coupled with model order reduction (MOR) techniques to reduce computing time [6]. However, the problem of boundary condition complexity at the machine or component level is still present in this solution.

In contrast, indirect (software) compensation of thermal errors at the tool centre point (TCP) is one of the most widely employed reduction techniques due to its cost-effectiveness and ease of application in the context of Industry 4.0 and intelligent machine tool [7]. Many strategies have been investigated to establish these models, e.g. transfer functions (TF) [8], multiple linear regressions (MLR) [9], artificial neural networks (ANN) [10], etc. The majority of the compensation models introduced in the literature have the potential to significantly reduce MT thermal errors. Therefore, further efforts should be focused on the applicability and verification of the approaches in real industrial conditions and environments.

An approach to thermal error modelling of a turning-milling centre in regard to various MT configurations was presented in [11]. In this research, the similar approach is critically evaluated by application on large grinding machine within the activity of wheel head with different grinding wheels clamped. The implementation and application capability of the composed models for thermal errors related to the parts of the MT stator parts and the axes of rotation are discussed.

The rest of the extended abstract is arranged as follows: In Section 2, the experimental setups and conditions are revealed. In Section 3, the modelling approach is described with the model structure applied on the measured data. Results are critically discussed. Conclusions and outlook for the further research are part of the last section.

2. Experimental setup and conditions

The MT for this research is a large grinding machine. The maximum diameter of a grinding wheel is 915 mm with rotation at 1350 rpm. The maximum diameter of a clamped workpiece is 1000 mm, length 4000 mm, and weight 9000 kg. The target machine was placed on the shop floor of a MT manufacturer. The shop floor is an open space without air conditioning equipped with a row of production machines. The environment could be considered stable with regard to years of manufacturer experience.

Basically, grinding machines are capable of simultaneous rotation realised in three components during working cycle: wheel head (rotation of grinding wheel), headstock and tailstock

(rotation of workpiece). This paper focuses on the impact of the wheel head on the thermal behaviour of the grinding machine. Two different grinding wheels mounted on the wheel head are considered. The experimental setup is depicted in Fig. 1. Figure 1 contains the positions of the temperature probes (the wheel head bearings temperature $T_{\text{wh bearings}}$ and the reference temperature $T_{\text{reference}}$ placed on the front bed). These temperatures are used as inputs to the thermal error compensation model. The displacements examined in the *X* direction between the headstock and the wheel head are also shown in Figure 1. Displacements were measured between static parts of both components ($\delta X_{\text{hs-wh stator}}$; informative value indicating mutual displacement of the static bodies of the headstock and the wheel head static bodies) and between their rotation axes of rotation ($\delta X_{\text{hs-wh rotor}}$; displacement with direct impact on the accuracy of the resultant workpiece accuracy).

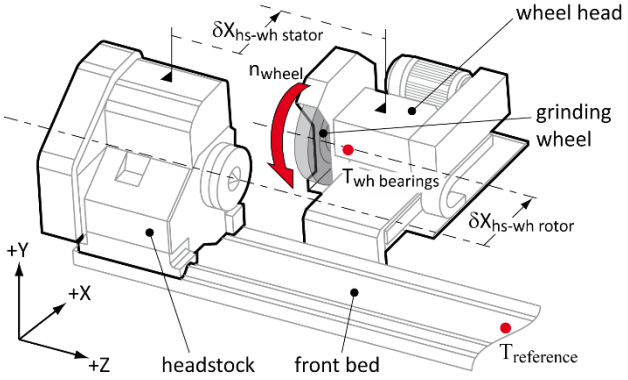

Figure 1. Experimental setup with wheel head activity of the wheel during grinding wheel rotation

Five experiments were carried out within the activity of the wheel head activity. The MT was equipped with two grinding wheels of different diameters. The experimental setups are summarised in the following table.

Table 1 Setup of realised tests

Test no.	**Grinding wheel diameter** [mm]	**Wheel rotation speed** [rpm]
1	915	1000
2		Variable
3		1350 (max.)
4	600	2000 (max.)
5		variable

Each experiment consisted of a part of transient behaviour between two thermodynamic equilibria (the MT in approximate balance with its surroundings and the MT steady state during heat source activity) ended after one work shift (6 to 8 hours) followed by a cooling phase (16 to 24 hours). The cooling process and as the well as grinding process were inactive during the experiments. The positions of the headstock and the wheel head remained unchanged within both experimental setups.

3. Training and testing of thermal error models

3.1. Modelling approach

The concept behind the modelling approach based on TFs lies in usage of a minimum of additional gauges, an open model structure that is easy to extend and modify [12] (advantageous for machine learning principles [13]), real-time application, and ease of implementation [12]. The mathematical apparatus is described in detail in [11].

The approximation quality of the simulated behaviour is expressed by global approach based on the least square method (*fit*; a percentage value where 100% would equal a perfect match of the measured and simulated behaviours) described in [14]

$$fit = \left(1 - \frac{\|\delta X_{mea} - \delta X_{sim}\|}{\|\delta X_{mea} - \overline{\delta X}_{sim}\|}\right) \cdot 100, \quad (1)$$

where δX_{mea} is the measured output (thermal deformation in the *X* direction), δX_{sim} is the simulated/predicted model output, and $\overline{\delta X}_{\text{sim}}$ expresses the arithmetic mean over time of the measured output.

The structure of the thermal error model using TFs is depicted in Fig. 2.

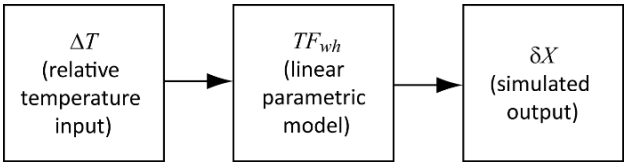

Figure 2. Structure of thermal error model

3.2. Results

A detailed profile of all realised tests in chronological order is shown in Fig. 3. Figure 3 contains changes in wheel rotation speeds over 5 days of testing. Test 1 is intended for training of thermal error models with the first wheel clamped (*D* = 915 mm). Test 2 verifies the models over quick speed start/stop changes realised in 30 min sequences, test 3 extends verification to maximal first wheel speed (1350 rpm). The wheel is changed (*D* = 600 mm) before test 5 starts with the maximum allowed speed for the second wheel. Tests 5 inspects linearity of MT thermo-mechanical behaviour over variation of second wheel rotation speed (the rotation changes every three hours).

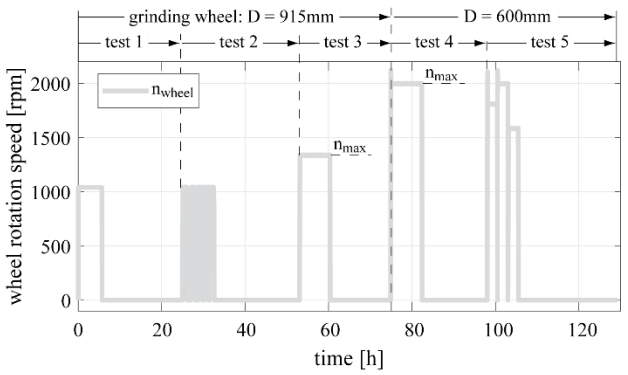

Figure 3. Grinding wheel speed profiles during test 1 to test 3 (wheel diameter 915mm) and test 4 and test 5 (wheel diameter 600mm)

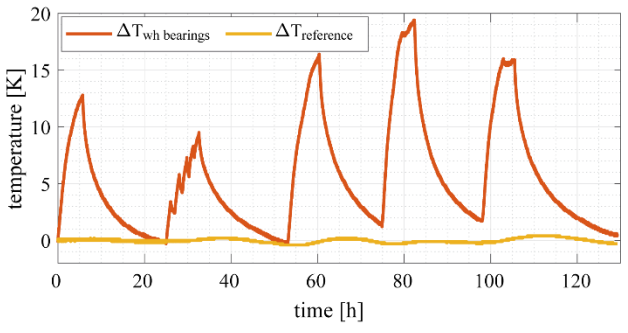

Figure 4. Relevant temperature behaviours during test 1 to test 5

The temperatures in relative coordinates (wheel head spindle bearings and reference temperature) measured over 5 days of testing are depicted in Fig. 4.

The measured (purple), the simulated (dashed black) and the residual relative displacements between static parts of the headstock and the wheel head bodies (black; difference between measured and simulated values) during the 120 hours of testing are shown in Fig. 5. Displacements are considered confidential and are listed dimensionless. The graph contains a highlighted area (from 0 to 21 hours; test 1, the first wheel clamped, 1000 rpm) dedicated to the model training. The only input into the thermal error model structure (see Fig. 2) is $\Delta T_{\text{wh bearings}}$. The order of the TF was selected based on the best *fit* value according to (1) during the ARX identification process (the TF used is second order). The stability of the identified TF is examined by the linear time-invariant (LTI) step response [14]. The training time is 21 hours. The rest of Fig. 5 depicts the verification of the model effectivity.

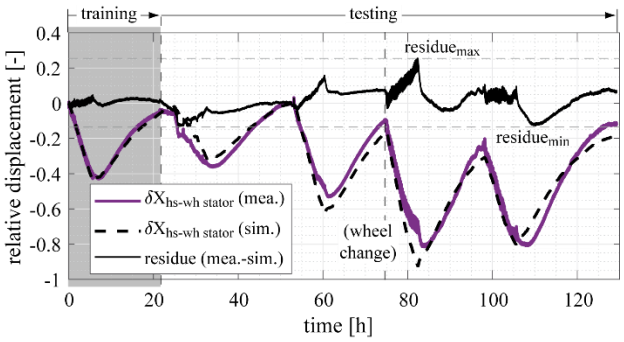

Figure 5. Measured, simulated, and residual displacements between static bodies of machine parts during test 1 to test 5

The measured (blue), the simulated, and the residual relative displacements between axes of rotation of headstock and the wheel head during overall testing are shown in Fig. 6. The training time (highlighted in Fig. 6), the model temperature input and the TF order are similar to the aforementioned model for static parts of MT components.

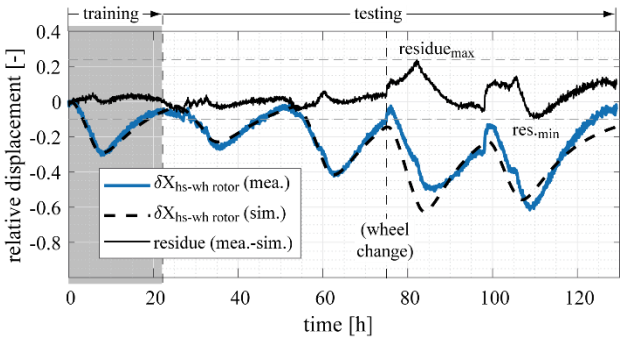

Figure 6. Measured, simulated, and residual displacements between axes of rotation of machine parts during test 1 to test 5

All results achieved results from the global approximation quality point of view (*fit*) are summarised in Table 2. Table 2 contains results from both individual tests and the model application for overall grinding machine behaviour.

Thermomechanical behaviour of the grinding machine under the specified conditions shows good linearity on the level of static parts level as presented in Fig. 6 and also in the upper part of Table 2 (overall *fit* value is 73% and evenly distributed over the individual tests).

Table 2 Results of model's effectivity during test 1 to test 5

Test no.	**1**	**2**	**3**	**4**	**5**	**Overall**
Model for static bodies						
fit [%]	87	55	54	58	73	73
Model for axes of rotation						
fit [%]	76	72	76	21	54	58

On the other hand, nonlinear behaviour can be observed during the approximation of displacements between axes of rotation, as seen in Fig. 6 and the lower part of Table 3 (overall *fit* value is 58%). The *fit* value deteriorates significantly during tests with the second grinding wheel clamped (tests 4 and test 5). It is probably caused due to different weights of grinding wheels, corresponding to different radial loads on the wheel head spindle bearings with a non-linear impact observed on this component level. The structure of the thermal error compensation model introduced in Fig. 3 should be upgraded (e.g. the model consisting of unique TFs for each grinding wheel and activation function controlled based on actually clamped grinding wheel) to improve its reliability. However, the industrial application of the upgraded model would still be limited. Firstly, the model functionality would depend on a control parameter (activation function) determining which part of the model should be currently active. Smooth connection of model parts during unsteady thermo-mechanical states could be problematic and the modelling complexity will be increased. Secondly, grinding machines are generally employed for precision finishing operations resulting in high surface quality. Active thermal compensation without in-process measurement can expose users to the risk of scrap production.

Herein, the implementation of an indicative model of thermal errors seems to be a suitable industrial approach instead of the real-time thermal error compensation model. In case of the indicative thermal error model, the calculated displacements are not superposed as an offset to the desired position values of the feed drive (no real-time compensation is carried out). However, the indicative thermal error model can provide valuable information to MT operator related to thermo-mechanical behaviour of the grinding machine, e.g. direction and relative magnitude of the non-stationary thermal errors. The model of thermal errors between static parts of the headstock and the wheel head can be considered as an indicative thermal error model for the investigated large grinding machine.

4. Conclusions

The main objective of the research presented in this paper is investigation of the industrial applicability of the compensation model on large grinding machines to enhance its accuracy by minimising the adverse impact of its thermo-mechanical behaviour. The machine was exposed to different thermal loads caused by clamping two different grinding wheels in the wheel head (915 mm and 600 mm in diameter *D*; no grinding process was involved). The relative displacements in the *X* axes of the wheel head and the headstock were measured in two positions: between static bodies of both components, providing only informative value of error directions and magnitude, and between their exes of rotation directly related to the workpiece accuracy. Two linear parametric single input single output models (based on transfer functions; each model related to one measured displacement position) were composed from the first experiment with the bigger wheel. Thermal error models were applied and analysed in four experiments with the following results:

- The thermal error models showed good long-term stability. However, the grinding machine was placed in shop floor with a stable ambient environment. An additional test with changeable ambient temperature should be carried out to prove the long-term stability of the model).
- The thermo-mechanical behaviour of the grinding machine at the level of static components is considered linear.
- The model for static parts of grinding machine components can be implemented in the control system of the grinding machine as an indicative model of thermal errors (the thermal error model is calibrated on experiments without cooling and grinding process which do not correspond to the real conditions during grinding operations).
- The industrial applicability of the indicative model lies mainly in providing valuable information to MT operator related to thermo-mechanical behaviour of the grinding machine (direction and relative magnitude of the non-stationary thermal error).
- The model composed for the approximation of thermal errors observed between the rotation axes of rotation showed a significant dependency on the clamped grinding wheel (diameter of the grinding wheel). The model should be upgraded to a single input multiple output structure, where each output approximates thermal errors caused by the activity of different grinding wheels clamped in the wheel head. However, the prolongation of model training period (model calibration) and modelling complexity limit the model's reliable industrial applicability as real-time thermal compensation without in-process measurement.

Consideration of a role of thermal error model in the MT energy efficient concept, involvement of the model in the principle of hybrid compensation (using both direct and indirect compensation strategies) and, last but not least, extension of the model applicability depending on the outputs from finite element analysis will be the focus of recent and follow-up research.

References

[1] Mayr J., et al., 2012, Thermal issues in machine tools, *CIRP Annals – Manufacturing Technology*, **61**(2), pp 771–791

[2] Grossmann K., et. al., 2015, Thermo-energetic design of machine tools: a systemic approach to solve the conflict between power efficiency, accuracy and productivity demonstrated at the example of machining production, Lecture Notes in Production Engineering, Springer, p. 260. ISBN 978-3-319-12624-1.

[3] Hellmich A., et al., 2018, Methods for analyzing and optimizing the fluidic tempering of machine tool beds of high performance concrete, In: *CIRP-sponsored 1st Conference on Thermal Issues in Machine Tools*, Dresden, Germany.

[4] Naumann C., et al., 2018, Hybrid correction of thermal errors using temperature and deformation sensors, In: *CIRP-sponsored 1st Conference on Thermal Issues in Machine Tools*, Dresden, Germany.

[5] Zimmermann N., et al., 2020, Extended discrete R-Test as on-machine measurement cycle to separate the thermal errors in Z-direction, In: *Proceedings of the euspen's Special Interest Group: Thermal Issues*, Aachen, Germany, pp 21-24.

[6] Hernández-Becerro P., et al., 2018, Model order reduction of thermal models of machine tools with varying boundary conditions, In: *CIRP-sponsored 1st Conference on Thermal Issues in Machine Tools*, Dresden, Germany.

[7] LIU K., et al., 2019, Intelligentization of machine tools: comprehensive thermal error compensation of machine-workpiece system, *The International Journal of Advanced Manufacturing Technology*, **102**(9-12), pp 3865-3877.

[8] Brecher C, et al., 2004, Compensation of thermo-elastic machine tool deformation based on control internal data. *CIRP Annals – Manufacturing Technology*, **53**(1), pp 299–304.

[9] Naumann C., et al., 2020, Comparison of basis functions for thermal error compensation based on regression analysis – a simulation based case study, *Journal of Machine Engineering,* **20**(4), pp 28–40.

[10] Mize C., et al., 2000, Neural network thermal error compensation of a machining center, *Precision Engineering*, **24**(4), pp 338–346.

[11] Mareš M., et al., 2020, Thermal error minimization of a turning-milling center with respect to its multi-functionality, *Int. J. of Automation Technology*, **4**(3), pp 475-483.

[12] Mareš M., et al., 2020, Thermal error compensation of a 5-axis machine tool using indigenous temperature sensors and CNC integrated Python code validated with a machined test piece, *Precision Engineering*, **66**(1), pp 21-30.

[13] Blaser P., et al., 2019, Long-term thermal compensation of 5-axis machine tools due to thermal adaptive learning control, *MM Science Journal*, **2019**(4), pp 3164-3171.

[14] Ljung L., 2015, System Identification Toolbox™ User's Guide, The MathWorks